

Multi-Robot Coordination Through Energy-based Dynamic Partitioning for Multi-Model Hot-Spot Sampling in Dynamic Environments

Kizito Masaba and Alberto Quattrini Li

Abstract—We propose a novel dynamic partitioning approach for robot coordination, which minimizes energy usage for robots on a multi-model hot-spot sampling mission in a dynamic environment. Real world environments have various disturbances, such as wind and water currents that impact a robot’s energy usage. Their magnitude and direction impede the robot’s navigation, which necessitates extra power intensive control. Thus, it is essential for robots to account for the impact of environmental dynamics in order to guarantee a successful multi-model hot-spot sampling mission. Existing partitioning methods such as Voronoi partitioning and Delaunay triangulation do not account for energy usage, rendering them inappropriate for balancing energy usage in a multi-robot coordination scenario. Thus, we propose an energy-conscious multi-model hot-spot sampling (*EMMS*) approach that is optimized for energy consumption at every step of the hot-spot sampling process by coordinating robots to ensure each robot minimizes energy usage across the robot team, and by computing energy efficient paths during sampling. *EMMS* partitions the environment according to the energy consumption of each robot such that a robot is assigned to a sub-region in which it consumes the least energy during sampling. It also ensures that robots navigate along paths that minimize energy usage by assessing the required energy for a given path using a realistic energy model that accounts for both the robot properties and environmental dynamics. We evaluate *EMMS* in a virtual environment that simulates realistic robot and environment dynamics. Our extensive experiments report over 30% higher energy savings by *EMMS* more than for traditional adaptive and non-adaptive methods.

I. INTRODUCTION

We propose a novel energy-conscious multi-robot coordination approach that minimizes energy usage of a robot team on a multi-model hot-spot sampling task in dynamic environments. With an energy model that accounts for both robot properties and environmental dynamics, this approach optimizes the informative path of a robot for both multi-model accuracy and energy conservation, thereby increasing the operating time of the robots for missions that require longer operating times such as multi-model hot-spot sampling. Multi-model hot-spot sampling refers to the process of sampling and modeling multiple properties of the environment simultaneously using robots in order to get more insights about a latent property of the environment. For instance, studying algal bloom in water quality monitoring [1] involves simultaneously sampling multiple chemical

The authors are in the Department of Computer Science, Dartmouth College, Hanover, NH, USA, 03755 {kizito.masaba.gr,alberto.quattrini.li}@dartmouth.edu

This work is supported in part by the Burke Research Initiation Award and NSF CNS-1919647, 2144624, OIA-1923004.

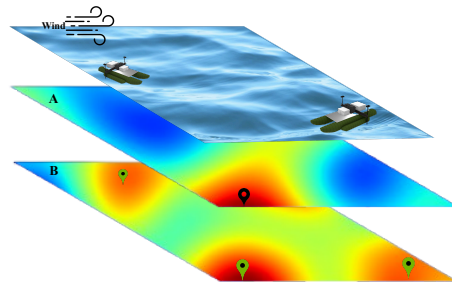


Fig. 1. Example Scenario: Given a team of robots, equipped with sensors that measure unknown spatial fields *A* and *B* in the target environment, required to identify and sample hot-spots of both fields, how can the robot team efficiently identify and sample all the hot-spots while conserving energy?

properties of a lake, such as chlorophyll, dissolved oxygen, turbidity, among us. Similarly, monitoring crop health in precision agriculture [2] involves measuring various chemical properties in the soil, such as nitrogen, phosphorus, organic matter, among others.

Whereas these properties are co-located, they are typically uncorrelated, implying that sampling hot-spots for one does not guarantee accurate sampling of others. Due to this independence, the number of hot-spot locations can increase dramatically as more properties are sampled since they may have highly diverse hot-spot locations as illustrated in Fig. 1. Therefore, it is essential to efficiently manage energy usage in order to guarantee success of such a mission.

Several methods have been proposed to guide robots on how to identify and sample hot-spots of a spatial field [3]–[6]. Generally, these methods build a model for a single spatial field using Gaussian Process Regression (GPR) [7] and define a data acquisition function that computes the significance of each location based on submodular information metrics [8] such as variance, mutual information [6], Fisher information [9], entropy [10], among others. The performance of a data acquisition function is evaluated based on how well it balances the exploration-exploitation trade off. One of the popular data acquisition functions is the upper confidence bound (UCB) [11], which balances this trade-off by computing a weighted sum of the model estimate and its corresponding uncertainty for a given location. This and other data acquisition functions prioritize sampling locations that improve model accuracy but do not explicitly account for the energy demands of visiting a target location. It is typically assumed that by minimizing makespan and traveled distance, energy consumption is implicitly minimized. While this is true in ideal environments, this may underestimate the energy losses in environments with various external disturbances, such as wind and water currents as in aquatic environments.

For instance, the literature [12], [13] shows that differential drive robots consume more energy during turns and when they travel full throttle for long periods of time or against the direction of wind and water currents. Hence, an efficient strategy for sampling a given location has to consider these costs in order to avoid premature termination of the hot-spot sampling mission.

Moreover, these approaches are designed for sampling hot-spots of a single phenomenon. Such approaches may also apply in multi-model hot-spot sampling if there is a high correlation among the target phenomena. However, such high correlations are not common in practice [14]–[16], which may lead to model inaccuracies and unexpectedly high energy usage in practical scenarios where multiple, uncorrelated phenomena need to be sampled accurately and simultaneously.

Hence, we propose an energy-conscious multi-model adaptive sampling (*EMMS*) technique that accounts for the uniqueness of each phenomenon and the energy constraints of the robot to enable accurate and reliable simultaneous sampling. *EMMS* incorporates both the estimated information for each model at a given location and energy cost for visiting the same location into data acquisition planning, ensuring that the technique not only balances the *exploration-exploitation* trade-off but also *exploration-energy* trade-off. In addition, *EMMS* implements an energy-conscious multi-robot coordination strategy that allows robots to explore the environment cost effectively by assigning each robot to sample sub-regions in which it minimizes energy usage. In summary, the main contribution of this work is two-fold:

- An energy-conscious multi-model hot-spot sampling approach for multi-model hot-spot sampling that minimizes energy usage to enable long monitoring cycles in dynamic environments.
- A novel energy-efficient environment partitioning strategy that enables a robot team to collectively maximize energy conservation by assigning each robot to sub-regions in which it minimizes energy usage.

This paper is structured as follows. Section II discusses related work focusing on environment modeling, path planning, and data acquisition methods. Section III formally states the sampling problem of focus. Section IV describes the environmental modeling, data acquisition functions, and energy models relevant to the proposed approach presented in Section V. Experiment setup, results and concluding remarks are presented in Section VI, VII, and VIII respectively.

II. RELATED WORK

The problem of identifying and sampling hot-spots of a spatial field has been widely studied in the literature [3]. Most of the proposed works address energy-related challenges in the *environment modeling* [17], [18] and *information gathering* steps of this task. In this section, we highlight some of the latest work proposed in both categories.

Environment modeling has been studied to address the scalability of GPR [7] models, which are commonly used in reconstructing spatial fields from samples. The most common

approaches in this category are the Mixture of Gaussian Process Experts (MGPs) [19]–[21] and environment partitioning [22]–[24]. The MGP model was introduced by Tresp *et al.* [20] as a model for active learning – another name for adaptive sampling – [3] problems. These methods model large spatial fields by aggregating local approximations obtained from a collection of models. For a comprehensive review of MGPs, please see the surveys from Liu *et al.* [19] and Yuksel *et al.* [25].

The works in *information gathering* can be categorized into the data acquisition work that proposes strategies for balancing the exploration-exploitation ratio and *motion planning*, which aims at finding the most energy efficient path for sampling. For *data acquisition*, [4], [26], [27] propose uncertainty sampling in order to minimize the mean squared error between model estimates and the target field. With this approach, regions of relatively high uncertainty are prioritized over those of low uncertainty but the magnitudes of estimates are not considered, making it inappropriate for identifying hot-spots. [11] propose the upper confidence bound, which balances this trade-off by quantifying information at any given location as a function of both the model uncertainty and the estimated value. With a good *exploration-exploitation* ratio parameter, this approach is efficient in identifying hot-spots. Other data acquisition functions include entropy, mutual information [28] and other sub-modular information-theoretic models. For a detailed review of these functions, the reader is referred to [3]. In multi-model sampling, these approaches assume that all the target fields share similar hotpot locations. This may not be the case in practice, especially when the spatial fields are not correlated. Our work accounts for this practical scenario when identifying hot-spots for each field.

On the other hand, several *information gathering* approaches have been proposed in the literature with the objective of obtaining a time optimal [29]–[31] or energy optimal [32] sampling plan in dynamic environments. One of the common approaches is identifying level set equations [33] that define an optimal path from source to target against existing environmental dynamics [29]. Other traditional methods rely on search algorithms such as Depth First Search (DFS) [34], Monte Carlo Tree Search (MCTS) [35], [36] and Dynamic Programming [37] to obtain the most energy efficient path to the target location. For instance, [38] applies MCTS to search for a high utility and energy efficient path for sampling ocean fronts with a custom multi-objective graph weighting function that is used to compute the weights of transects between a pair of endpoints on the graph. For a comprehensive review of these methods, the reader is referred to the motion planning surveys [39], [40]. Whereas some of these methods are energy efficient, they are mostly designed for identifying informative paths that maximize information gain rather than optimizing for energy conservation. They make general assumptions on the cost of navigating through environmental disturbances, but do not explicitly account for the vehicle’s energy consumption. In this work, we apply the graph search approach, but compute

the weight of sampling along a given transect using a realistic energy model that accounts for both the energy consumed by the vehicle mechanics amidst environmental disturbances.

III. PROBLEM FORMULATION

We assume a 2D environment, \mathcal{E} , with M unknown spatial fields, $Z = Z_1, \dots, Z_M$ such that the measurement for spatial field, Z_i at $x \in \mathcal{E}$ is $Z_i(x) = f_i(x) + \varepsilon_i$, where $\varepsilon_i \sim \mathcal{N}(0, \sigma_i^2), \forall i = 1, \dots, M$; a team of K differential drive robots, $R = \{r_1, \dots, r_K\}$ that can communicate with each other through long-range WiFi or radio devices, and are equipped with M sensors, $S = \{s_1, \dots, s_M\}$, such that sensor, s_i , measures spatial field Z_i . In addition, \mathcal{E} has external disturbances, like current or wind, that affect the robots energy consumption. The robots' task is to adaptively explore the environment in order to identify and sample hot-spots in Z within a predefined energy bound Λ . As each robot traverses the environment, it keeps track of the remaining energy, Λ^+ to ensure that the energy limit is not exceeded.

When the robot team is deployed, each robot collects data, $D = [X, Y_1, \dots, Y_M]$, where $X \subset \mathcal{E}$ are locations and Y_1, \dots, Y_M are the M field measurements collected at X such that sensor data for the i th field, $D_i = [X, Y_i]$. Assuming D_i is i.i.d, we can estimate the posterior distribution of the i th field, $f^i, \forall i = 1, \dots, M$ with a Gaussian Process Regression model, introduced in Section IV to obtain model collection, $F = [f^1, \dots, f^M]$. To enhance F , the goal for the robots is to sample unexplored locations and incorporate collected measurements into the the model estimates by first, identifying hot-spots in all the model estimates and then sampling them in the most energy efficient order.

IV. ENVIRONMENT, DATA ACQUISITION, AND ENERGY MODELS

A. Environment Modeling

Let X be a 2D vector of locations and y a vector of their corresponding measurements collected by the robot. X_* is a vector of test locations, whose measurements are to be estimated. Then, a GP model f for estimating X_* is drawn from a normal distribution defined as

$$f|X, y, X_* \sim \mathcal{N}(\mu, \sigma), \quad (1)$$

where the mean vector μ and covariance matrix σ are

$$\mu = K(X_*, X)[K(X, X) + \sigma_n^2 I]^{-1}y, \quad (2)$$

and

$$\sigma = K(X_*, X_*) - K(X_*, X)[K(X, X) + \sigma_n^2 I]^{-1}K(X, X_*) \quad (3)$$

respectively. The elements of the covariance matrix, $K(\cdot, \cdot)$, are given by a kernel function, which describes the spatial correlation between a pair of locations. We use a commonly used kernel because of its general applicability to different domains, the squared exponential (SE) [7], defined as

$$k_y(x_p, x_q) = \sigma_f^2 \exp\left(-\frac{(x_p - x_q)^2}{2l^2}\right) + \sigma_n^2 \sigma_{pq}, \quad (4)$$

where l is the length scale representing the function smoothness; σ_f^2 is signal variance determining the amplitude; σ_n^2 is the noise variance accounting for the estimate noise; and δ_{pq} is the Kronecker delta ($\delta_{pq} = 1$ if $p = q$, else $\delta_{pq} = 0$).

Using the SE kernel, a GP model is parameterized by $\theta = (\sigma_f^2, l, \sigma_n^2)$, which are determined from the data using Maximum Likelihood Estimation (MLE) [7], by maximizing

$$\log p(y|X, \theta) = -\frac{1}{2}y^T \Sigma_y^{-1}y - \frac{1}{2} \log |\Sigma_y| - \frac{n}{2} \log 2\pi \quad (5)$$

Given measurements of multiple spatial fields, we can simultaneously estimate them with the Multi-Task Gaussian Regression model [18], which uses GPR with a kernel that models correlations among the spatial fields, and outputs estimates (i.e, posterior mean and posterior variance) for each field. If the spatial fields are not correlated, we can model each spatial field separately using the GPR model defined in Equation (1). In this work, we model each field separately, since we assume that the spatial fields are not correlated.

B. Data Acquisition Function

GPR estimates can be used by the robot to determine the utility of sampling any given location, x . This utility is defined by the data acquisition function. One of the most commonly used data acquisition functions is the upper confidence bound (ucb) [11] defined as,

$$ucb(x) = \mu(X, y, x) + \omega \Sigma(X, y, x), \quad (6)$$

where ω is the exploration-exploitation tuning parameter, $\mu(X, y, x)$ and $\Sigma(X, y, x)$ are the posterior mean and variance at location x obtained from the GPR model. If ω is large (small), more (less) importance is given to locations with large posterior variances. Also, with a small ω , hot-spots (i.e., locations with maximum values) will be prioritized.

C. Energy Consumption

The work in [41] defines energy consumed by an autonomous surface vehicle (ASV) operating in an aquatic environment as the sum of its power dissipation P_{ASV} throughout the mission:

$$E = \sum P_{ASV} \Delta t \quad (7)$$

where Δt is the duration for which P_{ASV} is dissipated. P_{ASV} is the sum of two power components, defined as,

$$P_{ASV} = P_T + P_S, \quad (8)$$

where P_T and P_S is the power dissipated by the motors and electrical devices respectively. Note that P_T varies depending on the environmental disturbances, such as wind speed, V_w , its direction β_w , and water currents, V_c . For simplicity, we assume P_S is negligible. Consequently,

$$E \approx \sum P_T \Delta t \quad (9)$$

Given V_c , V_w , velocity of ASV, V_{ASV} , and the ASV specifications, P_T at any given time can be computed by:

$$P_T = \begin{bmatrix} m_{11} & 0 & 0 \\ 0 & m_{22} & 0 \\ 0 & 0 & m_{33} \end{bmatrix} \cdot \begin{bmatrix} \dot{u}_r \\ \dot{v}_r \\ \dot{r}_r \end{bmatrix} \cdot \begin{bmatrix} u_r \\ v_r \\ r_r \end{bmatrix} + \begin{bmatrix} 0 & 0 & -m_{22}v_r \\ 0 & 0 & m_{11}u_r \\ m_{22}v_r & -m_{11}u_r & 0 \end{bmatrix} \cdot \begin{bmatrix} u_r \\ v_r \\ r_r \end{bmatrix} \cdot \begin{bmatrix} u_r \\ v_r \\ r_r \end{bmatrix} + \begin{bmatrix} d_{11} & 0 & 0 \\ 0 & d_{22} & 0 \\ 0 & 0 & d_{33} \end{bmatrix} \cdot \begin{bmatrix} u_r \\ v_r \\ r_r \end{bmatrix} \cdot \begin{bmatrix} u_r \\ v_r \\ r_r \end{bmatrix} - \begin{bmatrix} \frac{1}{2}\rho_a \cdot A_{Fw} \cdot c_x \cdot V_w^2 \cdot \cos(\phi - \beta_w) \\ \frac{1}{2}\rho_a \cdot A_{Lw} \cdot c_y \cdot V_w^2 \cdot \cos(\phi - \beta_w) \\ 0 \end{bmatrix} \cdot \begin{bmatrix} u_r \\ v_r \\ r_r \end{bmatrix} \quad (10)$$

with:

$$V_r = V_{ASV} - V_c = \begin{bmatrix} u_r \\ v_r \\ r_r \end{bmatrix} = \begin{bmatrix} u - V_{cx} \cos \phi - V_{cy} \sin \phi \\ v - V_{cx} \sin \phi - V_{cy} \cos \phi \\ r \end{bmatrix}.$$

Each term is defined as follows:

- $m_{11} = m + 0.05$, where m is the weight of the ASV
- $m_{22} = m + 0.5\rho\pi D^2 L$, where $\rho \approx 1025 \text{Kg m}^{-3}$ is the water density, D is the ASV submerged depth and L is length of the ASV.
- $m_{33} = \frac{m(L^2 + W^2) + 0.5(0.1md^2 + \rho\pi D^2 L^3)}{12}$, where W is the width of the ASV and d is the distance between its motors.
- $d_{11} = \frac{F_{Th}}{u_{\max}}$, where $F_{Th} = F_{Th1} + F_{Th2}$ is the sum of left (F_{Th1}) and right (F_{Th2}) thruster forces, u_{\max} is the maximum surge velocity of the ASV.
- $d_{22} = \frac{-m_{11}u_r}{2r_{\max}}$
- $d_{33} = \frac{F_N d}{2r_{\max}}$, $F_N = F_{Th1} - F_{Th2}$ is the difference between left and right thruster forces, and r_{\max} is the maximum rotation speed.
- $[c_x, c_y]$ is the center of gravity that depends on the shape of the ASV.
- A_{Fw} and A_{Lw} are the frontal and lateral projected areas.
- ϕ and β_w are the ASV heading and wind direction.
- $\phi - \beta_w$ is the wind's angle of attack relative to the ASV.
- $V_c = [V_{cx}, V_{cy}]$, where V_{cx} , V_{cy} is the water current speed in x and y directions respectively.
- ρ_a is the air density, where $\rho_a \approx 1.184 \text{Kg m}^{-3}$ at warm temperatures.

In this work, we use the ASV (catobot 2.0) designed in our lab [42] whose specifications are given as $m = 90 \text{Kg}$, $L = 2.5 \text{m}$, $W = 1.57 \text{m}$, $D = 0.865 \text{m}$, $[c_x, c_y] = [1.47 \text{m}, 1.42 \text{m}]$, $u_{\max} = 2 \text{m/s}$, $r_{\max} = 4 \text{rad}$, $d = 1.5 \text{m}$, $A_{Fw} = 1.42 \text{m}^2$, $A_{Lw} = 1.4 \text{m}^2$. Given the wind speed and direction, $[V_w, \beta_w]$, and water current speed, $V_c = [V_{cx}, V_{cy}]$ and ASV velocity, $V_{ASV} = [u, v, r]$ at any given time, we can compute P_T with Equation (10) and sum it up to estimate the energy consumed by an ASV during the mission.

V. ENERGY-CONSCIOUS SIMULTANEOUS FIELD SAMPLING ALGORITHM

After robot deployment, hot-spot sampling has two iterative steps, environment modeling and data acquisition. In this

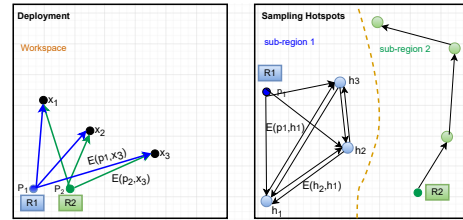


Fig. 2. Illustration of the proposed method. Left: Deployment of robots. The coordinator robot samples arbitrary locations, X in the workspace and generates a bipartite graph between the robot poses and X . The weight of each edge, (x_i, x_j) on the graph is defined by the estimated energy, $E(x_i, x_j)$ consumed by the robot to travel from x_i to x_j under existing disturbances. Right: Robot, $R1$ identifies one hot-spot from each field, h_1, h_2, h_3 within its assigned sub-region and plans to sample each of them. A directed graph is generated, where the nodes are the robot pose and hot-spots, and the edge weights are the estimated energy consumed by the robot when navigating from one edge endpoint to another. From the graph, a Hamiltonian path is computed using a Traveling Salesperson Problem (TSP) solver. The robot samples the hot-spots by following the resulting path.

section, we present the proposed energy-conscious approach that ensures each step is done in an energy efficient manner as illustrated in Fig. 2.

A. Energy-conscious Robot Deployment

Initially, robots localize into the target environment, measure the environmental disturbances and exchange their global poses. One robot on the team is arbitrarily assigned to coordinate the deployment. The coordinator robot selects sample locations as deployment location candidates and identifies the most optimal location to deploy each robot. Optimality is determined by the potential amount of energy consumed by the robot to navigate from its pose to a target location, which can be computed by the energy model described in Section IV-C. To determine the most optimal target location for each robot, the coordinator robot generates a complete bipartite graph, $G = (U, V, \kappa)$, where $(p_i \in U, v \in V)$ is an edge that maps robot pose, p_i to a target location, v and its weight, $w_{iv} \in \kappa$ is the estimated energy required by robot i to navigate to v . From G , optimal assignments can be computed by finding the minimum energy cost edge $(u_i, v), \forall i = 1, \dots, K$. With this approach, we ensure that each robot consumes minimal energy at deployment. The coordinator robot then shares deployment locations to each robot in accordance with this assignment.

B. Environment Modeling and Energy-Conscious Sampling

As a robot navigates the environment, it simultaneously collects data for all the target spatial fields. This data is used to estimate the distribution of each field across the workspace. We use the *GPR* model defined in Section IV-A to estimate these distributions from collected data. Since we assume no correlation between the spatial fields, we model each field independently to obtain the model collection, F . The model collection is continuously updated after every data collection cycle.

From F , a robot identifies hot-spots that need to be sampled using the Upper Confidence Bound (UCB) described in Section IV-B. Since F is updated after every sampling cycle, a robot selects one hot-spot with the highest UCB from each model, f^i for sampling in order to balance sampling across

all fields. Hence, we select M hot-spots for sampling in every cycle and compute an energy efficient path that traverses the selected hot-spots.

To obtain an energy-efficient path, we create a connected directed graph $\mathcal{H} = (S, T, W)$, where S is the set of nodes representing the hot-spot locations, $(s, t) \in T$ is an edge on \mathcal{H} and $e_{st} \in W$ is the weight of (s, t) , defined as the estimated energy consumed when navigating from node s to t . Given \mathcal{H} , the most energy efficient path is the Hamiltonian tour, which can be obtained using a Traveling Salesperson Problem (TSP) solver. Once the path is obtained, the robot proceeds to traverse the tour and collect data, which is then incorporated into the model. This process repeats until the energy consumption, Λ^+ reaches a critical point.

C. Energy-Conscious Partitioning

For the multi robot case, we further minimize energy usage by coordinating the robot team such that each robot only samples and models a sub-region which minimizes its energy usage. Specifically, we partition the environment such that each sub-region is sampled with minimal energy requirements. For any location $x \in \mathcal{E}$, robot i is assigned to x if it has sufficient energy and consumes the least energy to navigate to x from its current target location compared to others. Thus, the region assigned to robot i is specified as:

$$V_i = \{x \in \mathcal{E} : \arg \min_i E(x_i, x, V_d) = i, \quad (11)$$

$$s.t. \Lambda_i^+ > 0, \forall i = 1, \dots, K\},$$

where $E(x_i, x, V_d)$ is the total energy consumed when navigating from its current target location, x_i to x amidst environmental disturbances, V_d , and Λ_i^+ is the remaining energy on robot i . At the beginning of every sampling cycle, robots exchange collected data and their next target locations to ensure that each robot on the team is maintaining an up-to-date model collection and is sampling in appropriate sub-regions.

VI. EXPERIMENTS

We evaluate the proposed approach (labeled as *EMMS*) in a lake environment $500\text{m} \times 325\text{m}$ that has up to 4 unique spatial fields, *SF1*, *SF2*, *SF3* and *SF4* (Fig. 3). The spatial fields are synthetically generated to represent chemical properties of lake water, such as Chlorophyll-A, PH, Conductivity, Nitrogen. All these chemical properties are essential in water quality monitoring against algal bloom growth in lakes. We also specify wind speed, $V_w = 4\text{m/s}$ and its direction, $\beta = 0^\circ$ (direction of wind in North East is from North West in summer [43]), and water current velocity, $V_c = [0.035\text{m/s}, 0.035\text{m/s}]$ to simulate realistic disturbances in the lake during sampling in US North Eastern Lakes, as average wind speed of a gentle breeze [44] and average water current speed in the summer [45].

We use *EMMS* to sample hot-spots of the above spatial fields using robot teams of 4 different sizes, namely 1, 2, 3 and 4. Each robot is equipped with sensors that simultaneously sample the fields with signal-to-noise ratio of 5% and a

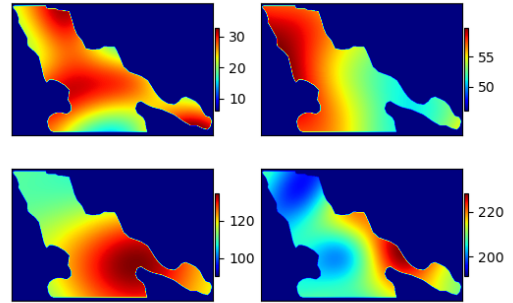


Fig. 3. Test spatial fields top left: *SF1*, top right: *SF2*, bottom left: *SF3* and bottom right: *SF4*. Note that all spatial fields have their hot-spots at unique locations.

battery capacity of 220 Wh when fully charged. We randomize experiments by simulating 5 different battery levels at the beginning of deployment, namely 100%, 80%, 60%, 40% and 20%. The robots are assumed to have uniform battery charge levels at deployment. The environment, robots, and their sensors are simulated in Stage [46], a lightweight simulator for multi robot systems. Each experiment terminates when either the battery discharges to critical levels or after 1200 s.

Finally, we evaluate *EMMS* against six(6) other methods to assess its different components and its performance against traditional methods. These include 1) *MMS*, which samples hot-spots from all fields (as in *EMMS*) but does not account for energy usage in planning and coordination. 2) *EMS*, which samples all fields based on a single field and accounts for energy consumption in its coordination (as in *EMMS*). 3) *MS*, which samples all fields based on a single field but does not account for energy consumption (as in *MMS*), and 4) *VMMS*, which applies dynamic partitioning [23] using Voronoi Partitioning and samples hot-spots from all fields but does not account for energy usage in planning and coordination. In addition, we evaluate it against 5) vertical (*LMV*) and 6) horizontal (*LMH*) boustrophedon sampling [47], with an inter-lap spacing that is optimized for a full coverage while enforcing energy constraints. Note that all methods that are guided by a single field use *SF1* as their primary target field.

The performance metrics for evaluation include *Reconstruction Error* as Root Mean Squared Error (RMSE) for each spatial field, *hot-spot error* (i.e., RMSE between ground truth hot-spots and corresponding measurements in estimates), *average energy usage*, and *average traveled distance* by each robot at the end of the mission.

VII. RESULTS AND DISCUSSION

First, we evaluate energy usage for each method to assess the effect of applying an energy-conscious adaptive sampling approach in hot-spot sampling. Results of *battery usage* (Fig. 4) show that energy-conscious methods, *EMS* and *EMMS* show a steady drop of battery usage as the robot team size increases and the usage drops to almost 30% more than the non energy-conscious methods. On the other hand, methods that are not energy-conscious, *MMS*, *VMMS*, *MS*,

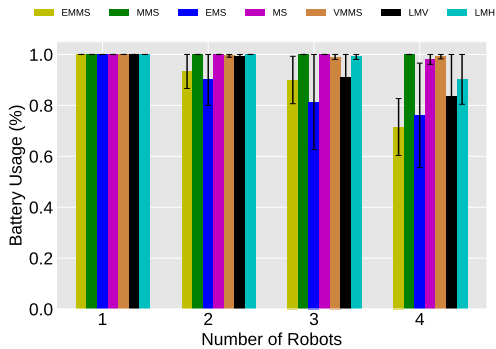


Fig. 4. *Battery usage* for each robot on different team sizes. energy-conscious methods, *EMMS* and *EMS* consume the least energy, followed by *LM** methods. Non energy adaptive methods, have the highest energy usage.

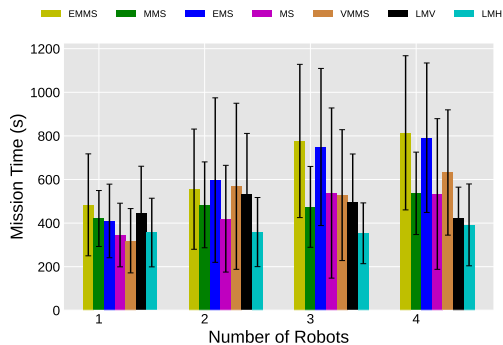


Fig. 5. *Mission time* for each method according to robot size. The period of operation steadily increases with robot team size for energy-ware methods, *EMMS* and *MS*.

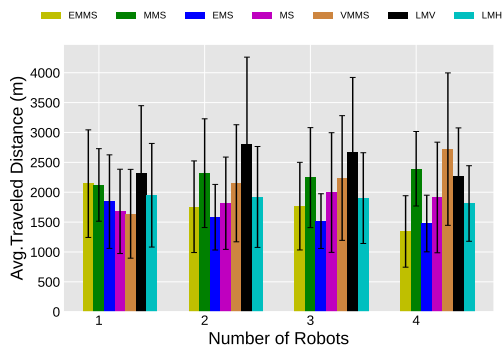


Fig. 6. *Average traveled distance* by a robot for each method according to robot size. The travel distance for energy-conscious methods steadily drops as the robot team size increases.

LMV, and *LMH* are generally not affected by the increase in robot size, despite the multi-robot coordination and data sharing they enforce. The high energy-scalability exhibited by energy-conscious methods allows them to operate longer (see Fig. 5), which makes them advantageous in long-term monitoring missions. Moreover, energy-conscious methods have the lowest *average traveled distance* compared to their counterparts as shown in Fig. 6. This demonstrates the effectiveness of using energy usage for robot coordination, as it enables robots to exploit nearby hot-spots in a bid to conserve energy, which consequently minimizes their traveled distance. The UCB method tends to prioritize far unexplored regions due to the GPR kernel used, which leads to long distance travels. However, this is evidently mitigated as energy usage is incorporated into the data acquisition

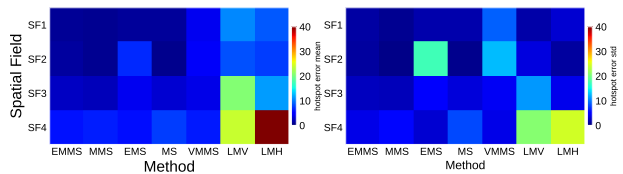


Fig. 7. Heatmap showing mean and standard deviation of *hot-spot error* in hot-spot measurements for all spatial fields. Overall, all the adaptive methods perform more efficiently across all spatial fields compared to the non-adaptive methods.

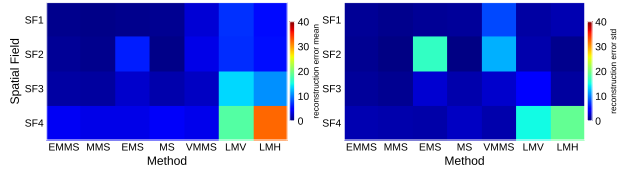


Fig. 8. Heatmap showing mean (left) and standard deviation (right) of *reconstruction error* in the estimates of all spatial fields by each method. Overall, all the adaptive methods perform more efficiently across all spatial fields compared to the non-adaptive methods.

process.

Secondly, we evaluate the efficiency of *EMMS* in identifying and sampling hot-spots for all the fields by analyzing the *hot-spot error* (Fig. 7). Overall, all adaptive methods accurately reconstruct all spatial fields with minimal error. However, non-adaptive methods have relatively higher *hot-spot error* in all fields as they miss sampling regions that are not traversed by the predefined lawn mower tour. Similarly, adaptive methods accurately reconstruct all fields as exhibited by the low *reconstruction error* in Fig. 8 since they are able to successfully sample hot-spots, whereas non-adaptive methods have higher *reconstruction error* error due to their inability to exhaustively sample all the significant locations, thanks to their rigid sampling profile.

Overall, the results demonstrate the significance of using adaptive methods in hot-spot sampling and also highlight the need to account for energy usage at every step of the hot-spot sampling process.

VIII. CONCLUSION

We proposed an energy-conscious multi-model hot-spot sampling (*EMMS*) technique that enables robots to simultaneously reconstruct multiple spatial fields in aquatic environments amidst environmental disturbances, such as wind and water currents. With *EMMS*, robots use the upper confidence bound (UCB) data acquisition model to identify hot-spots for each target spatial field and an energy model to sample hot-spots in the most energy efficient manner. To further conserve energy, the robot team coordinates to ensure that each robot samples a sub-region that minimizes its energy usage. Experiments demonstrate *EMMS* technique's effectiveness in sampling hot-spots for all the fields and its efficiency in conserving energy. Moreover, they highlight the benefits of accounting for energy usage in hot-spot sampling.

Potential future directions for this work is to explore ways of integrating the two conflicting objectives, energy conservation and information gathering into one energy-conscious sub-modular function for data acquisition purposes. Finally, we also plan to implement *EMMS* in sampling various

chemical properties of the lake that are observed in our long-term water quality monitoring project.

REFERENCES

- [1] S. Behmel, M. Damour, R. Ludwig, and M. Rodriguez, "Water quality monitoring strategies—a review and future perspectives," *Science of the Total Environment*, 2016.
- [2] S. Fountas, N. Mylonas, I. Malounas, E. Rodias, C. Hellmann Santos, and E. Pekkeriet, "Agricultural robotics for field operations," *Sensors*, 2020.
- [3] A. T. Taylor, T. A. Berrueta, and T. D. Murphey, "Active learning in robotics: A review of control principles," *Mechatronics*, 2021.
- [4] A. Blanchard and T. Sapsis, "Informative path planning for anomaly detection in environment exploration and monitoring," *Ocean Engineering*, 2022.
- [5] A. Blanchard and T. Sapsis, "Bayesian optimization with output-weighted optimal sampling," *Journal of Computational Physics*, 2021.
- [6] A. Singh, A. Krause, C. Guestrin, and W. J. Kaiser, "Efficient informative sensing using multiple robots," *Journal of Artificial Intelligence Research*, 2009.
- [7] C. E. Rasmussen, "Gaussian processes in machine learning," in *Summer school on machine learning*, Springer, 2003.
- [8] A. Krause and C. Guestrin, "Near-optimal observation selection using submodular functions," in *AAAI*, 2007.
- [9] A. D. Wilson, J. A. Schultz, and T. D. Murphey, "Trajectory synthesis for fisher information maximization," *IEEE Transactions on Robotics*, 2014.
- [10] S. Otte, J. Kulick, M. Toussaint, and O. Brock, "Entropy-based strategies for physical exploration of the environment's degrees of freedom," in *Proc. IROS*, IEEE, 2014.
- [11] R. Marchant and F. Ramos, "Bayesian optimisation for informative continuous path planning," in *Proc. ICRA*, IEEE, 2014.
- [12] D. Ventura, A. Bonifazi, M. F. Gravina, and G. D. Ardizzone, "Unmanned aerial systems (UASs) for environmental monitoring: A review with applications in coastal habitats," *Aerial Robots-Aerodynamics, Control and Applications*, 2017.
- [13] H. Niu, Z. Ji, A. Savvaris, and A. Tsourdos, "Energy efficient path planning for unmanned surface vehicle in spatially-temporally variant environment," *Ocean Engineering*, 2020.
- [14] N. E. Ray, M. A. Holgerson, M. R. Andersen, *et al.*, "Spatial and temporal variability in summertime dissolved carbon dioxide and methane in temperate ponds and shallow lakes," *Limnology and Oceanography*, 2023.
- [15] S. McGowan, R. K. Juhler, and N. J. Anderson, "Autotrophic response to lake age, conductivity and temperature in two west greenland lakes," *Journal of Paleolimnology*, 2008.
- [16] T. Wu, G. Zhu, M. Zhu, H. Xu, Y. Zhang, and B. Qin, "Use of conductivity to indicate long-term changes in pollution processes in lake taihu, a large shallow lake," *Environmental Science and Pollution Research*, 2020.
- [17] H. Liu, J. Cai, and Y.-S. Ong, "Remarks on multi-output gaussian process regression," *Knowledge-Based Systems*, 2018.
- [18] E. V. Bonilla, K. Chai, and C. Williams, "Multi-task gaussian process prediction," *Proc. NeurIPS*, 2007.
- [19] H. Liu, Y.-S. Ong, X. Shen, and J. Cai, "When Gaussian process meets big data: A review of scalable GPs," *IEEE transactions on neural networks and learning systems*, 2020.
- [20] V. Tresp, "Mixtures of Gaussian processes," *Proc. NeurIPS*, 2000.
- [21] K. Masaba and A. Quattrini Li, "Multi-robot adaptive sampling based on mixture of experts approach to modeling non-stationary spatial fields," in *Proc. MRS*, IEEE, 2023.
- [22] G. P. Kontoudis and D. J. Stilwell, "Decentralized nested Gaussian processes for multi-robot systems," in *Proc. ICRA*, IEEE, 2021.
- [23] S. Kemna, J. G. Rogers, C. Nieto-Granda, S. Young, and G. S. Sukhatme, "Multi-robot coordination through dynamic Voronoi partitioning for informative adaptive sampling in communication-constrained environments," in *Proc. ICRA*, IEEE, 2017.
- [24] L. Wu, M. Á. García García, D. Puig Valls, and A. Solé Ribalta, "Voronoi-based space partitioning for coordinated multi-robot exploration," *Journal of Physical Agents*, 2007.
- [25] S. E. Yuksel, J. N. Wilson, and P. D. Gader, "Twenty years of mixture of experts," *IEEE transactions on neural networks and learning systems*, 2012.
- [26] D. J. MacKay, "Information-based objective functions for active data selection," *Neural computation*, 1992.
- [27] D. A. Cohn, "Neural network exploration using optimal experiment design," *Neural networks*, 1996.
- [28] A. Krause, A. Singh, and C. Guestrin, "Near-optimal sensor placements in Gaussian processes: Theory, efficient algorithms and empirical studies," *Journal of Machine Learning Research*, 2008.
- [29] T. Lolla, P. F. Lermusiaux, M. P. Ueckermann, and P. J. Haley, "Time-optimal path planning in dynamic flows using level set equations: Theory and schemes," *Ocean Dynamics*, 2014.
- [30] R. Singh and N. Bussa, "Path planning using shi and karl level sets," in *International ICST Conference on Robot Communication and Coordination*, 2010.
- [31] T. Cecil and D. E. Marthaler, "A variational approach to path planning in three dimensions using level set methods," *Journal of Computational Physics*, 2006.
- [32] P. Tokekar, N. Karnad, and V. Isler, "Energy-optimal trajectory planning for car-like robots," *Autonomous Robots*, 2014.
- [33] S. Osher and R. P. Fedkiw, "Level set methods: An overview and some recent results," *Journal of Computational physics*, 2001.
- [34] R. Tarjan, "Depth-first search and linear graph algorithms," *SIAM journal on computing*, 1972.
- [35] M. A. Nguyen, K. Sano, and V. T. Tran, "A monte carlo tree search for traveling salesman problem with drone," *Asian Transport Studies*, 2020.
- [36] G. Best, O. M. Cliff, T. Patten, R. R. Mettu, and R. Fitch, "Decentralised monte carlo tree search for active perception," in *Algorithmic Foundations of Robotics XII: Proceedings of the Twelfth Workshop on the Algorithmic Foundations of Robotics*, Springer, 2020.
- [37] A. Mingozzi, L. Bianco, and S. Ricciardelli, "Dynamic programming strategies for the traveling salesman problem with time window and precedence constraints," *Operations research*, 1997.
- [38] S. McCammon, G. Marcon dos Santos, M. Frantz, *et al.*, "Ocean front detection and tracking using a team of heterogeneous marine vehicles," *Journal of Field Robotics*, 2021.
- [39] J. R. Sánchez-Ibáñez, C. J. Pérez-del-Pulgar, and A. García-Cerezo, "Path planning for autonomous mobile robots: A review," *Sensors*, 2021.
- [40] H.-Y. Zhang, W.-M. Lin, and A.-X. Chen, "Path planning for the mobile robot: A review," *Symmetry*, 2018.
- [41] W. Touzout, Y. Benmoussa, D. Benazzouz, E. Moreac, and J.-P. Diguët, "Unmanned surface vehicle energy consumption modelling under various realistic disturbances integrated into simulation environment," *Ocean engineering*, 2021.
- [42] M. Jeong, M. Roznere, S. Lensgraf, A. Sniffen, D. Balkcom, and A. Quattrini Li, "Catabot: Autonomous surface vehicle with an optimized design for environmental monitoring," in *Global Oceans 2020: Singapore-US Gulf Coast*, IEEE, 2020.
- [43] K. Klink, "Climatological mean and interannual variance of united states surface wind speed, direction and velocity 1," *International Journal of Climatology: A Journal of the Royal Meteorological Society*, 1999.
- [44] N. N. W. Service, *Estimating wind*. [Online]. Available: <https://www.weather.gov/pqr/wind>.
- [45] B. Sahoo, M. Mao, and M. Xia, "Projected changes of water currents and circulation in lake michigan under representative concentration pathways scenarios," *Journal of Geophysical Research: Oceans*, 2021.
- [46] R. Vaughan, "Massively multi-robot simulation in stage," *Swarm intelligence*, 2008.
- [47] H. Choset and P. Pignon, "Coverage path planning: The boustrophedon cellular decomposition," in *Field and service robotics*, Springer, 1998.